2732 *Biochemistry* **2010,** *49,* 2732–2740
DOI: 10.1021/bi9016654

BIOCHEMISTRY
including biophysical chemistry & molecular biology
Article

An RNA Aptamer with High Affinity and Broad Specificity for Zinc Finger Proteins[†]

Tristen C. Weiss, Gary G. Zhai, Simran S. Bhatia, and Paul J. Romaniuk*

Department of Biochemistry and Microbiology, University of Victoria, P.O. Box 3055, Victoria, BC V8W 3P6, Canada

Received September 23, 2009; Revised Manuscript Received February 22, 2010

ABSTRACT: A class of RNA aptamers that demonstrates a high affinity for a large variety of C_2H_2 zinc finger proteins was isolated from a library of random RNA sequences by the zinc finger protein TFIIIA. These aptamers have one or more copies of the consensus sequence GGGUGGG, which is part of a putative hairpin loop in the proposed structure of the most abundant aptamer, RNA1. Binding of zinc finger proteins to RNA1 relies upon zinc-dependent folding of the protein, the affinity of an individual protein for RNA1 being determined by the number of tandem zinc finger motifs. The properties of RNA1 were compared to the properties of two other aptamers from the same selection experiment: RNA21, which binds to some but not all zinc finger proteins tested, and RNA22, which binds only to the 5S rRNA binding zinc finger proteins TFIIIA and p43. The binding of three different zinc finger proteins to RNA1 was compared, and the results indicate that the RNA1−protein interaction occurs by several distinct mechanisms. Mutagenesis of RNA1 confirmed that the GGGUGGG consensus sequence presented in a hairpin conformation is required for high-affinity binding of zinc finger proteins.

Zinc finger proteins carry out diverse functions in the cell, generally involving specific interactions with DNA, RNA, or protein ligands (*1*, *2*). The presence of a tandem array of C_2H_2 zinc fingers within a previously uncharacterized coding sequence or protein is generally considered to be indicative that the protein will bind to a specific sequence of DNA and in some way act to regulate transcription of genes. Some members of this class of zinc finger proteins are multifunctional, which requires that the zinc finger domains in these proteins interact with more than one class of ligand. For example, transcription factor IIIA (TFIIIA) binds to the promoter of the 5S rRNA gene (*3*−*6*) and also binds to 5S rRNA to form a storage ribonucleoprotein particle in the cytoplasm of immature oocytes (*7*−*10*). The DNA and RNA ligands for TFIIIA have quite distinct conformations, and the protein utilizes the first three of its nine zinc fingers to mediate binding to DNA and the central zinc fingers to mediate binding to RNA (*11*−*22*). WT1, a protein with a smaller zinc finger domain, accommodates interactions with DNA and RNA by using an overlapping array of key amino acids (*23*, *24*). The neuronal-specific transcription factor REST uses eight tandem zinc fingers to bind to the same sequence of base pairs in the promoters of target genes, and in a short double-stranded RNA that modulates its regulatory activity (*25*). The *Xenopus* protein Zfa is a member of a class of proteins that bind to double-stranded RNA with C_2H_2 zinc fingers (*26*, *27*) that are spaced farther apart with much longer linkers than those found in proteins like TFIIIA. The overall fold of the RNA binding domain of this class of proteins is different from that of the proteins with closely spaced zinc fingers (*28*), suggesting it has been optimized for binding to double-stranded RNA rather than the typical C_2H_2 zinc finger protein that binds to DNA and/or a folded single-stranded RNA.

The conformational parameters of the DNA double helix and the RNA double helix differ significantly in areas particularly important for protein binding (*29*). Of primary importance are the dimensions of the major groove: in the typical B-type DNA double helix, the major groove is optimal for the docking of an α-helix from a protein in such a way to allow for the formation of noncovalent bonds between side chains on the amino acids and functional groups on the base pairs that allow for readout of the base sequence. In comparison, the major groove in the typical A-type RNA double helix is too narrow and deep to allow for a meaningful interaction between amino acid residues on an α-helix and the sequence-discriminating functional groups on the bases of the RNA. Single-stranded RNA molecules that adopt three-dimensional shapes may form more open structures in regions consisting of noncanonical base pairing, allowing for the formation of direct contacts between the α-helix of a zinc finger and the RNA bases (*30*). In addition, tipping of the amino-terminal region of a zinc finger α-helix is a strategy that allows for the formation of specific contacts with RNA bases.

Given these differences in the conformations of DNA and RNA, it is remarkable that at least some zinc finger proteins are able to form specific interactions with both classes of nucleic acids. After enriching a library of random RNA sequences for aptamers that form high-affinity complexes with TFIIIA, we determined that the two most abundant aptamers demonstrated high affinity for zinc finger proteins in general (*31*). One of these aptamers (RNA1) bound to all zinc finger proteins that we tested with affinities in the subnanomolar range. To understand the properties of this aptamer in more detail, we have undertaken a study that compares the binding of this broad-specificity aptamer to TFIIIA with the binding of a highly specific aptamer (RNA22) to the same protein. We have also compared the interaction of several different zinc finger proteins with RNA1 to understand the common and divergent features of their interactions with this aptamer. Finally, we used site-directed mutagenesis to identify key sequence and structural elements in RNA1 involved in the formation of high-affinity interactions with a broad range of zinc finger proteins.

[†]This work was supported by a grant from the Natural Sciences and Engineering Research Council of Canada.

*To whom correspondence should be addressed. Telephone: (250) 721-7088. Fax: (250) 721-8855. E-mail: pjr@uvic.ca.

 Published on Web 02/22/2010

MATERIALS AND METHODS

Bacterial Strains and Plasmid Vectors. Plasmid vectors pET16b and pET30a were used to express recombinant wild-type and mutant zinc finger proteins in *Escherichia coli* strain BL21 DE3 using methods that have been described elsewhere (*32*−*34*).

Construction of Zinc Finger Protein Expression Vectors. Construction of plasmid vectors used to express *Xenopus* TFIIIA and the zinc finger peptides YY1 and ZFY6 has been described previously (*31*).

Expression and Purification of Recombinant Zinc Finger Proteins. Preparations of N-terminally His-tagged zinc finger proteins were conducted as described previously (*32*). Recombinant *Xenopus* TFIIIA was purified by ion exchange chromatography on BioRex-70 (*33*). Protein purity was confirmed by polyacrylamide gel electrophoresis, and the concentration of each protein preparation was determined by the method of Bradford (*35*).

Radiolabeling of RNA Ligands. Preparation of radiolabeled 5S rRNA and selected RNA aptamers by in vitro transcription was conducted as described previously (*36*).

Equilibrium Binding of RNAs to Zinc Finger Proteins. The apparent association constants for the binding of radiolabeled RNAs to zinc finger proteins were determined using a double-filter binding assay (*37*). The binding buffer consisted of 20 mM Tris-HCl (pH 7.5, 20 °C), 5 mM $MgCl_2$, 100 mM KCl, 10 μM $ZnCl_2$, 0.5 mM tris(2-carboxyethyl)phosphine hydrochloride, 100 μg/mL BSA, and 1 μg/mL polyA. When the effects of altering binding conditions such as temperature, pH, divalent salt concentration, or monovalent salt concentration were being investigated, the binding buffer was altered accordingly.

The affinity of each zinc finger protein for RNA was determined using three or more independent assays. Apparent dissociation constants (K_d) for the binding of the mutant and wild-type proteins to RNA were calculated by fitting the data to a simple bimolecular equilibrium model using the general curve fitting function of Kaleidagraph (Synergy Software, Reading, PA) and the following equation:

$$\frac{[\text{RNA}-\text{protein}]}{[\text{RNA}]_{\text{total}}} = \frac{[\text{protein}]_{\text{total}}}{[\text{protein}]_{\text{total}} + K_d} \quad (1)$$

where $[\text{RNA}]_{\text{total}} \ll K_d$ and $[\text{RNA}-\text{protein}]/[\text{RNA}]_{\text{total}}$ is reported as the fraction of RNA bound. Values of the association constant (K_a) were derived as the reciprocal of the measured K_d values and are reported as the mean of three independent determinations with the associated standard deviations. We determined relative affinities by dividing the apparent K_a for the mutant RNA by the apparent K_a for the wild-type RNA determined in parallel. The errors for relative affinities are given by the expression $\sigma = [(\sigma_1/M_1)^2 + (\sigma_2/M_2)^2]^{1/2} \times M_2/M_1$, where M_1 and M_2 are the association constants for the wild-type and mutant proteins, respectively, and the σ values are the corresponding standard deviations for these determinations.

Analysis of the Thermodynamic Parameters of RNA Binding by Zinc Finger Proteins. The contribution of enthalpy ($\Delta H°$) and entropy ($\Delta S°$) to the free energy of RNA binding by zinc finger proteins was determined from the temperature dependence of the apparent K_a using van't Hoff plots of $\ln(K_a)$ versus $1/T$. In those cases where enthalpy was independent of temperature, the plot was linear and was analyzed using eq 2:

$$\ln(K_a) = -(\Delta H°/RT) + \Delta S°/R \quad (2)$$

For the interaction of TFIIIA with RNA21 and RNA22, the plots were significantly nonlinear and were analyzed using eq 3 (*38*), where the change in molar heat capacity is represented by $\Delta C°_{p,\text{obs}}$. T_H and T_S are the temperatures at which enthalpy and entropy, respectively, make no contribution to the free energy of formation of the TFIIIA−RNA complex (*38*).

$$\ln(K_a) = (\Delta C°_{p,\text{obs}}/R)[T_H/T - \ln(T_S/T) - 1] \quad (3)$$

The data in the van't Hoff plots were fit to eq 3 using the general curve fitting function of Kaleidagraph version 3.0 to solve for $\Delta C°_{p,\text{obs}}$, T_H, and T_S, and these parameters were then used to calculate the contributions of enthalpy and entropy to the free energy of formation of the protein−RNA complex as a function of temperature using eqs 4 and 5 (*38*).

$$\Delta H° = \Delta C°_{p,\text{obs}}(T - T_H) \quad (4)$$

$$T\Delta S° = T \times \Delta C°_{p,\text{obs}} \times \ln(T/T_S) \quad (5)$$

RESULTS

Basic Requirements of Zinc Finger Binding to RNA1. RNA1 (Figure 1A) was the most abundant aptamer selected from a random library of RNA molecules using the bait protein TFIIIA (*31*) and contains the GGGUGGG consensus motif found in two-thirds of the aptamers in the enriched library. RNA1 shows virtually no specificity for a particular zinc finger protein: all of the zinc finger proteins tested exhibited high affinity for RNA1. To investigate the properties of this aptamer further, we started by determining whether the high affinity RNA1 has for a broad range of zinc finger proteins relies upon the proper folding of the zinc finger domain. As the results in Figure 1B show, TFIIIA, the YY1 zinc finger domain peptide, and the ZFY6 peptide consisting of zinc fingers 6−13 of the ZFY protein all bind to RNA1 with high affinity when zinc is included in the buffer used to refold the purified proteins. When the zinc in the buffer is replaced with EDTA, which prevents the coordination of zinc to the cysteine and histidine side chains of the zinc finger motif, the proteins are no longer capable of binding to RNA1.

The initial observation that RNA1 is unselective in binding to zinc finger proteins indicated that there might be a relationship between the length of a zinc finger protein and its affinity for RNA1. The affinities of a series of zinc finger peptides of differing length, derived from a variety of proteins, were determined. As the number of zinc fingers in the proteins tested increased, there was a linear increase in the logarithm of the apparent K_a of binding to RNA1 (Figure 2). For zinc finger proteins consisting of three to nine zinc fingers, the increase in the free energy of binding ($\Delta\Delta G°$) is 0.282 ± 0.032 kcal/mol for each additional zinc finger. This result confirms that the structure and sequence of RNA1 allow for the formation of one or more contacts to each zinc finger of the protein that binds.

Comparison of the Equilibrium Binding of TFIIIA to RNA1, RNA21, and RNA22. To understand how RNA1 might act as a broad-spectrum ligand for zinc finger proteins, we compared the effects of different binding conditions on the interaction of the three most abundant RNA aptamers (RNA1, RNA21,

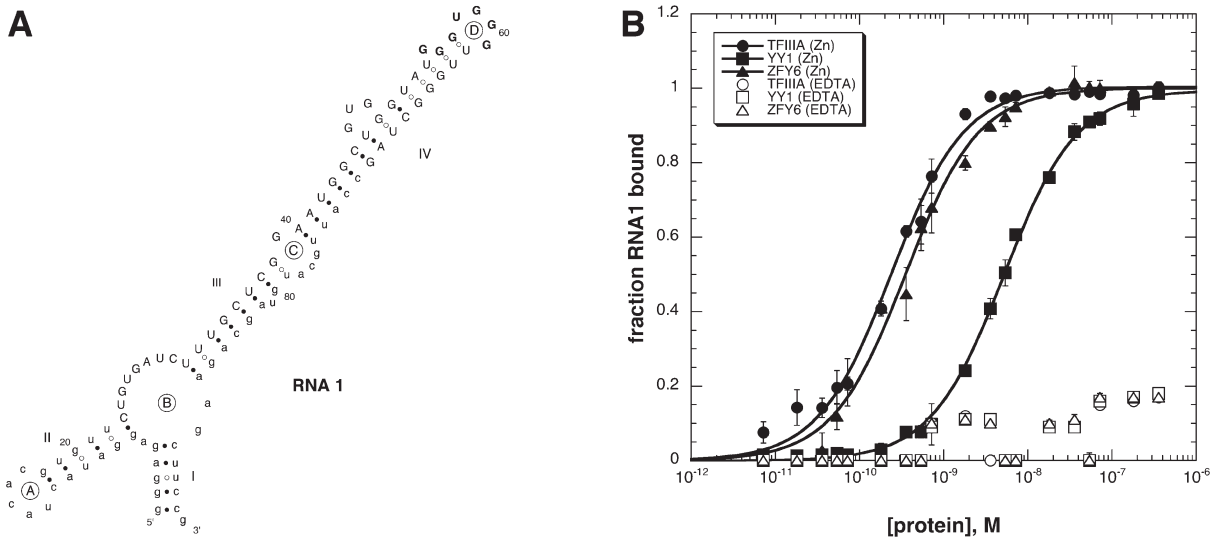

FIGURE 1: (A) Secondary structure of RNA1 predicted by *mfold* at 20 °C using version 2.3 parameters (*52*, *53*). Nucleotides selected from the random 50mer region are shown in uppercase, and fixed priming sequences are shown in lowercase. The consensus GGGUGGG sequence is shown in bold. (B) Equilibrium binding of three zinc finger proteins to RNA1 in the presence and absence of zinc.

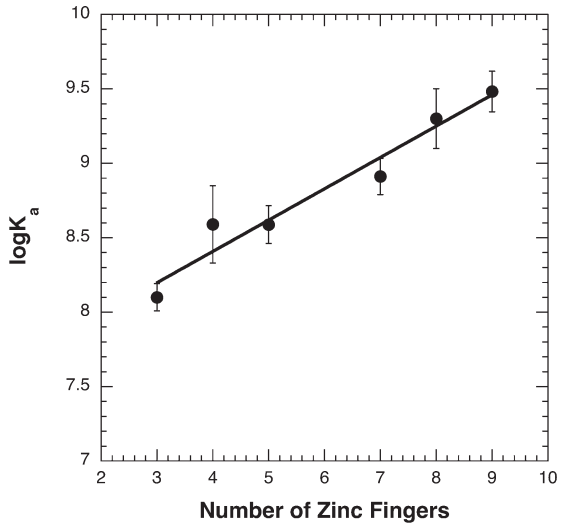

FIGURE 2: Relationship between the apparent association constant for binding to RNA1 and the number of tandem zinc finger motifs in the protein partner. The data points for three, five, and seven zinc fingers are the means of three independent determinations of K_a for a single peptide in each case derived from the ZFY protein, with the error bars representing the standard deviation of the mean. The data points for four, eight, and nine zinc fingers are the mean K_a values determined in triplicate for five, three, and two different zinc finger proteins, respectively, with the error bars representing the standard deviation of the mean.

and RNA22) with the original bait protein TFIIIA. These aptamers have high affinities for TFIIIA but differ in the degree of specificity they have for this protein compared to any other zinc finger protein (*31*).

The response of the apparent association constant to increases in monovalent salt concentration in the assay buffer is a measure of the relative contribution of ionic interactions to the overall free energy of binding. In the case of a DNA−protein interaction, the data obtained can be used to calculate this contribution to free energy, and the number of ionic contacts formed between the protein and the DNA (*39*−*41*). Such a detailed analysis of an RNA−protein interaction is not feasible, because it requires too many untested assumptions. However, the data for RNA−protein interactions can be compared on a qualitative basis. When the binding of the three RNA aptamers to TFIIIA is measured as a function of monovalent salt concentration, it is apparent that the less selective aptamers RNA1 and RNA21 are less sensitive to changes in salt concentration than is the highly specific aptamer RNA22 (Figure 3A). One can reasonably conclude that ionic interactions contribute more to the free energy of the TFIIIA−RNA22 interaction than they do to the interaction of TFIIIA with either RNA1 or RNA21.

Magnesium ions participate in the folding of RNA structures through diffuse interactions with the phosphate backbone, and site-specific interactions important for tertiary folding (*42*). Site-specific interactions of magnesium with an RNA can be important for the formation of a high-affinity, high-specificity complex with a protein (*43*). Diffuse interactions of magnesium with the phosphate backbone may facilitate interactions with a protein or compete with a protein for the formation of ionic interactions (*44*). A comparison of the effects of increasing Mg^{2+} ion concentration on the binding of TFIIIA to RNA1, RNA21, and RNA22 showed no significant differences among the three RNA aptamers (Figure 3B). The three interactions all show a modest decrease as the divalent metal ion concentration increases from 1 to 20 mM, consistent with a competition between the proteins and magnesium for binding to the phosphate backbone of the aptamers.

To determine the involvement of titratable groups in the interactions of the three RNA aptamers with TFIIIA, the effect on binding affinity of varying buffer pH within the range of 6.0−9.0 was determined (Figure 3C). The interaction of RNA1 with TFIIIA has a fairly flat pH profile from 6.5 to 9.0, with the affinity increasing at pH 6.0, suggesting that the pH optimum for this interaction may lie below this pH. In comparison, the interaction of RNA21 with TFIIIA has a broad pH optimum between 6.0 and 7.5 with affinity decreasing at pH > 7.5. RNA22 exhibits a profile similar to that of RNA21 between pH 6.5 and 9.0 but also exhibits a distinct decrease in TFIIIA affinity at pH 6.0. Since the three RNA aptamers each display different pH profiles for the binding of TFIIIA, it would be tempting to conclude that the important titratable groups are found on each RNA. However, it is equally feasible that different titratable

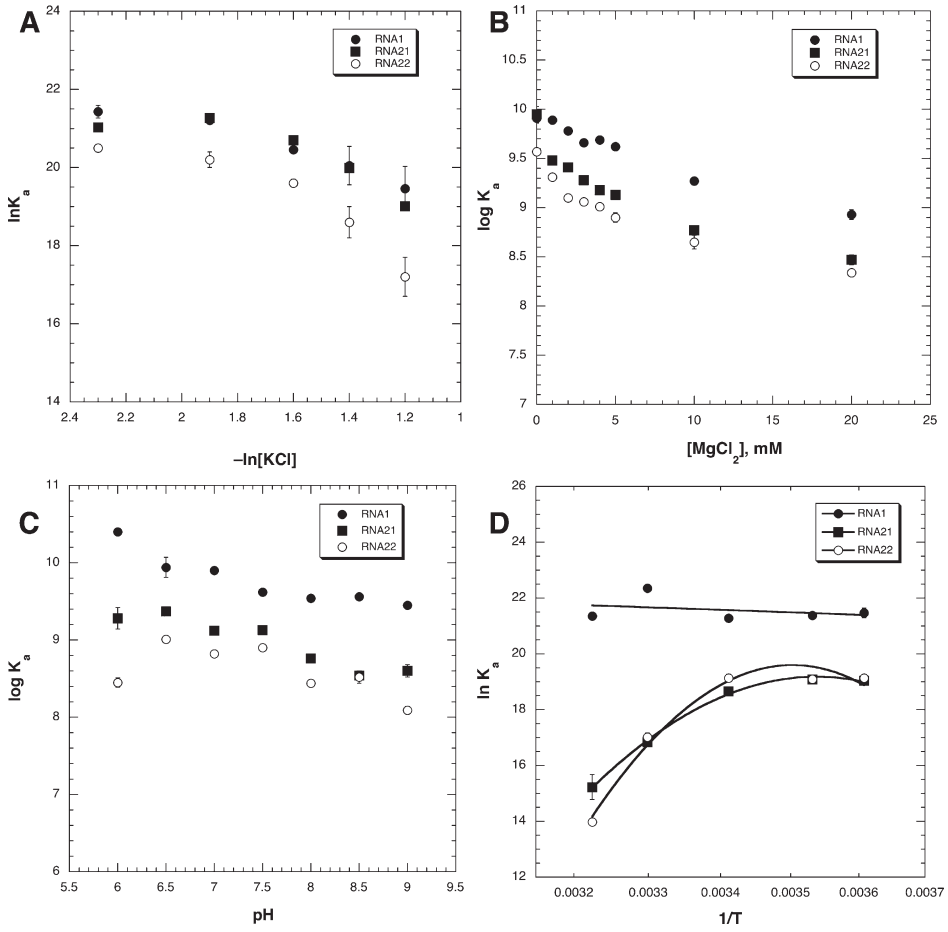

FIGURE 3: (A) Effect of monovalent salt concentration on the affinity of TFIIIA for RNA1, RNA21, and RNA22. (B) Effect of divalent salt concentration on the affinity of TFIIIA for RNA1, RNA21, and RNA22. (C) Effect of pH on the affinity of TFIIIA for RNA1, RNA21, and RNA22. (D) Effect of assay temperature on the affinity of TFIIIA for RNA1, RNA21, and RNA22. The data points represent the mean of two independent determinations of K_a, with the error bars representing the standard deviation of the mean.

groups on TFIIIA are involved in the interaction of the protein with each of the RNAs.

The relative contributions of enthalpy and entropy to the free energy of binding provide another insight into differences in the mechanisms of RNA−protein interactions. A comparison of the temperature dependence of the binding affinities for the interaction of TFIIIA with the three aptamers is shown in Figure 3D. The interaction of RNA1 with TFIIIA is best described by a linear relationship between log K_a and temperature (eq 2), whereas the interactions of RNA21 and RNA22 with TFIIIA are distinctly nonlinear, indicating that the enthalpy of the interaction is temperature-dependent (eq 3). This characteristic could indicate that RNA21 and RNA22 have a folded structure with inward-facing hydrophobic faces that fold away upon protein binding. Such an unfolding could also result in the presence of fewer condensed cations in the complex, which would be supported by the slight differences observed in the sensitivities of the three TFIIIA−aptamer interactions to the concentrations of monovalent and divalent salts in the binding buffer. The thermodynamic parameters derived from fitting the data to the appropriate equations are listed in Table 1. It is clear that at the standard assay temperature of 20 °C, the interaction of TFIIIA with RNA1 is driven entirely by a favorable entropy, while the interactions of the protein with RNA21 and RNA22 are driven entirely by favorable enthalpy terms.

Previous studies of the interactions of TFIIIA with 5S rRNA and RNA22 identified key amino acids through the analysis of the effects of site-directed mutations in the protein on RNA binding affinities (*31*, *45*, *46*). The affinities of these same mutant TFIIIA proteins for RNA1 were measured to compare the effects of the mutations on RNA1 binding with those previously measured for RNA22 binding. The series of Xw mutants of TFIIIA are chimeric proteins in which specific regions of TFIIIA are replaced with sequences derived from unrelated zinc finger protein WT1 (Figure 4) (*45*). The data in Figure 4 indicate that binding of TFIIIA to the highly specific RNA22 aptamer relies upon amino acids in zinc fingers 4 and 6, whereas binding of TFIIIA to the RNA1 aptamer that has a high affinity for a broad spectrum of zinc finger proteins is not significantly affected by mutations that substitute all or parts of zinc fingers 4−7 with heterologous finger sequences derived from WT1. The mutations in most cases slightly increased the affinity of the resulting chimeric TFIIIA protein for RNA1, with complete replacement of the α-helix of finger 6 resulting in a small 2.5-fold decrease in affinity (Figure 4). These data clearly illustrate the nonspecific, high affinity that RNA1 has for zinc finger proteins, regardless of whether they are natural, wild-type proteins or chimeras of two unrelated proteins.

Comparison of the Equilibrium Binding of Unrelated Zinc Finger Proteins to RNA1. To understand further how RNA1 might act as a broad-spectrum ligand for zinc finger proteins, we compared the effects of different binding conditions on the interaction of three different zinc finger proteins with RNA1. The TFIIIA, ZFY6, and YY1 proteins chosen for this

Table 1: Thermodynamic Constants for the Interaction of RNA Aptamers with Zinc Finger Proteins

	$\Delta C°_{p,obs}$[a] (kcal/mol)	T_H[a] (K)	T_S[a] (K)	$\Delta H°$(20 °C) (kcal/mol)	$\Delta S°$(20 °C) (cal deg^{-1} mol^{-1})
			Interaction of TFIIIA with Three RNA Aptamers		
RNA1	–	–	–	1.8 ± 3.1[b]	49.1 ± 10.5[b]
RNA21	-1.9 ± 0.2	282.7 ± 1.0	288.4 ± 0.5	-19.6 ± 2.0[c]	-29.8 ± 3.6[d]
RNA22	-3.4 ± 0.7	285.5 ± 1.8	288.8 ± 1.3	-25.4 ± 6.8[c]	-48.6 ± 15.0[d]
			Interaction of RNA1 with Three Zinc Finger Proteins		
TFIIIA	–	–	–	1.8 ± 3.1[b]	49.1 ± 10.5[b]
YY1	–	–	–	-10.0 ± 2.0[b]	4.2 ± 7.0[b]
ZFY6	–	–	–	-7.1 ± 2.8[b]	16.6 ± 9.6[b]

[a]Values were calculated from nonlinear regression analysis of the data in Figures 3 and 5 using eq 3 and are reported ± the standard error of regression. [b]Values were calculated from nonlinear regression analysis of the data in Figures 3 and 5 using eq 2. [c]Values were calculated using eq 4 and incorporating errors from $\Delta C°_{p,obs}$ and T_H. [d]Values were calculated using eq 5 and incorporating errors from $\Delta C°_{p,obs}$ and T_S.

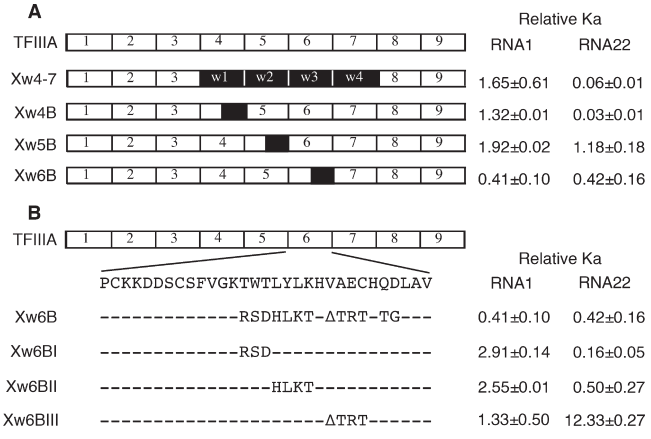

FIGURE 4: Comparison of the effects of site-directed mutations of TFIIIA on RNA1 and RNA22 binding affinities. (A) Effects of scanning mutations created using zinc finger sequences from unrelated protein WT1 (black boxes). (B) Amino acid sequence of zinc finger 6 along with the scanning mutations created within the α-helix of this finger. Relative binding affinities were determined from three independent determinations, as outlined in Materials and Methods.

comparison have only the zinc finger motif in common, differing in the number of zinc fingers and the amino acid sequences of the zinc fingers. These three proteins are members of the C_2H_2 class of zinc finger proteins, each having a mix of fingers that strictly conform to, and others that deviate slightly from, the canonical motif and therefore should be quite similar in structure.

As the data in Figure 5A show, the interactions of TFIIIA and ZFY6 with RNA1 are less sensitive to monovalent salt concentration (a decrease in ln K_a upon going from the lowest salt concentration to the highest) than the interactions of YY1 with RNA1 (a decrease in ln K_a of 3 upon going from the lowest salt concentration to the highest). This result implies that the contribution of ionic contacts to the free energy of binding a zinc finger protein to RNA1 is not a constant but depends upon the nature of the zinc finger sequences in each individual protein.

Upon comparison of the binding of the three zinc finger proteins to RNA1 as a function of increasing divalent metal ion concentration, ZFY6 shows the same modest decrease in apparent K_a as TFIIIA does (Figure 5B). However, the interaction of YY1 with RNA1 is weakened more sharply at the introduction of $MgCl_2$ into the binding buffer at 1−2 mM before being modestly weakened as the concentration of the salt increases beyond this. Perhaps RNA1 undergoes a conformational change at a low $MgCl_2$ concentration that decreases the affinity of YY1 for the aptamer.

The comparison of the pH profiles for binding of TFIIIA, YY1, and ZFY6 to RNA1 yielded some significant differences (Figure 5C). The interaction of ZFY6 with RNA has an optimal pH range of 6.0−7.5, with a significant decrease in affinity occurring at pH ≥8.0. The pH profile for YY1 shows that the pH optimum for this protein may lie below 6.0, as observed for TFIIIA. However, unlike TFIIIA, the interaction of YY1 with RNA1 shows a sharp decrease in affinity at pH ≥8.0. The discontinuity observed at pH 8 for ZFY6 and YY1 may indicate two overlapping pH profiles, one for the protein partner and the other for RNA1. Regardless of whether the key titratable groups involved in each of these interactions lie within the RNA or protein, the results demonstrate the flexibility of RNA1 in accommodating the formation of different bonding contacts to the various zinc finger proteins.

A comparison of the temperature dependence of the interaction of the three zinc finger proteins with RNA1 was also conducted (Figure 5D). The data for YY1 and ZFY6 were initially analyzed using both eqs 2 and 3. The enthalpy and entropy terms at 20 °C provided by both analyses were very similar, but the best fit to the data was obtained with eq 2. As the data in Table 1 show, the interactions of YY1 and ZFY6 with RNA1 differ in thermodynamic terms from the interaction of TFIIIA with RNA1. The TFIIIA−RNA1 interaction is driven by a large favorable entropy, while the interactions of YY1 and ZFY6 are driven by large favorable enthalpy terms. In the case of YY1, entropy is either slightly favorable or unfavorable for complex formation, whereas formation of the ZFY6−RNA1 complex is favored by entropy as well as enthalpy.

To understand what features of RNA1 are required for binding to zinc finger proteins with high affinity and broad specificity, we utilized the predicted secondary structure (Figure 1A) as a guide in designing site-directed mutations of the RNA. One obvious target for mutagenesis is the GGGUGGG sequence found in RNA1 and two-thirds of the unique sequences found in the enriched aptamer library. This sequence forms loop D at the end of helix IV in the predicted RNA1 structure. This loop is closed by five noncanonical base pairs. Regions with these types of base oppositions such as the "loop E" region of 5S rRNA form unique local structures with a network of hydrogen bonding interactions between the opposing strands (*30*, *47*). Seven mutants of RNA1 were created to test the importance of the consensus sequence, and the structural presentation of that sequence

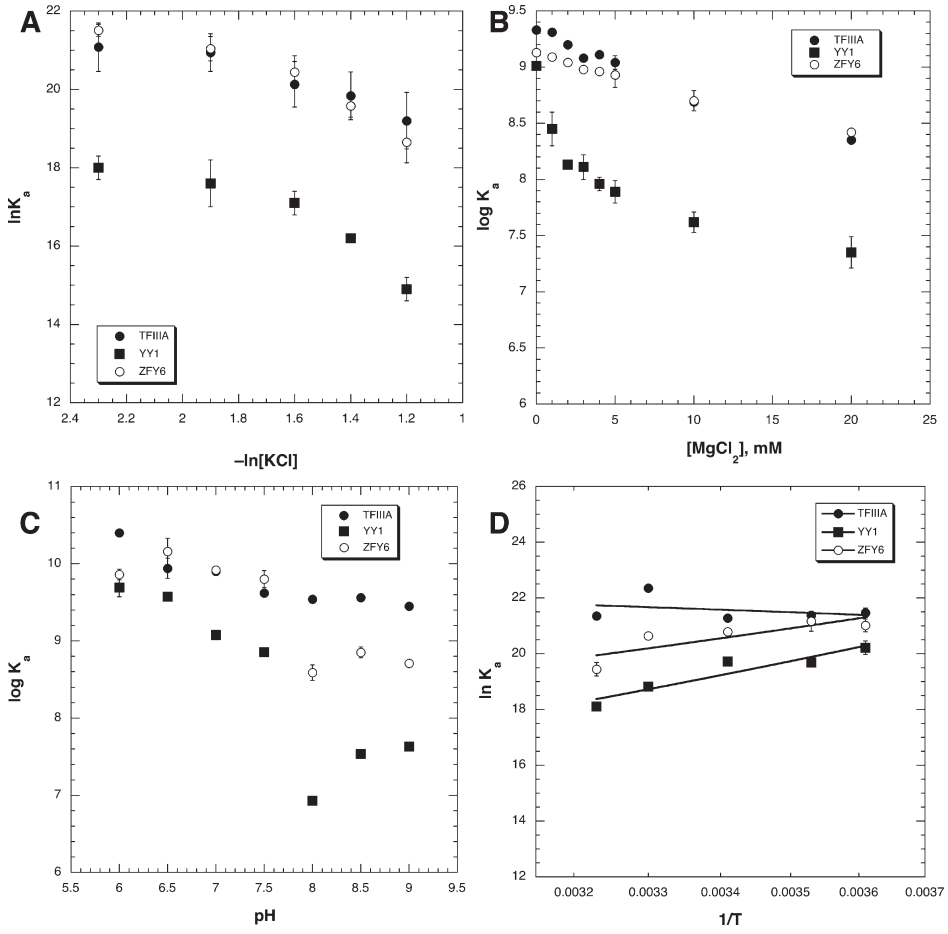

FIGURE 5: (A) Effect of monovalent salt concentration on the affinity of TFIIIA, YY1, and ZFY6 for RNA1. (B) Effect of divalent salt concentration on the affinity of TFIIIA, YY1, and ZFY6 for RNA1. (C) Effect of pH on the affinity of TFIIIA, YY1, and ZFY6 for RNA1. (D) Effect of assay temperature on the affinity of TFIIIA, YY1, and ZFY6 for RNA1. The data points represent the mean of two independent determinations of K_a, with the error bars representing the standard deviation of the mean.

within the context of the full-length RNA1 molecule (Figure 6). Mutant M1 replaces the GGGUGGG consensus sequence with the AAAGAAA sequence but maintains the formation of the loop D structure. This mutation weakens binding of zinc finger proteins TFIIIA, YY1, and ZFY6 by 62.5−500-fold. In comparison, mutations M2 and M3, which alter the identity of the base pairs closing loop D but retain the GGGUGGG consensus sequence, have only modest effects on the binding of the three zinc finger proteins (Figure 6).

The first G of the consensus sequence is predicted to adopt an extrahelical "bulged" conformation in the RNA1 structure. The importance of this putative conformation of the G was tested in mutants M4 and M5, which convert this G into a base-paired form either by extending helix IV by a base pair (M4, Figure 6) or by causing a shift in the position of the consensus sequence within helix IV by altering the base pairs preceding this G (M5, Figure 6). Both of these alterations result in significant decreases in the affinity of RNA1 for the zinc finger proteins, the largest effect being observed for mutant M4 (Figure 6). Mutants M6 and M7 were designed to test the importance of the noncanonical base pairing arrangement predicted to occur in helix IV immediately preceding the consensus sequence. Mutant M7 is predicted to adopt the wild-type conformation of RNA1, and this mutation decreases the affinity for the zinc finger proteins by a modest 2.6−7.9-fold (Figure 6). This result for mutant M7 suggests that the noncanonical base pairs formed between nucleotides 52−54 and nucleotides 64−66 adopt a structure that contributes to the binding of the zinc finger proteins. Mutant M6 is predicted to adopt a structure that maintains loop D but alters the conformation of helix IV in the region of the first base of the consensus sequence (Figure 6). This G is predicted to be part of a G-C base pair, and the UAU sequence of nucleotides immediately preceding it is predicted to form an extrahelical loop rather than being involved in the noncanonical base pairing found in this region of wild-type RNA1. The rearrangement of the bases in this region of helix IV results in a 5.8−11.2-fold decrease in affinity for the zinc finger proteins, again suggesting that the unique structural features of this region of wild-type RNA1 are part of the binding determinants for the zinc finger proteins.

DISCUSSION

Our initial intent in selecting RNA aptamers with high affinity for TFIIIA was to use them to test whether the related 5S rRNA binding protein p43 shared a common structural framework for RNA binding. The three most abundant sequences in the enriched library of RNA aptamers all had similar high affinities for TFIIIA but exhibited distinct characteristics in terms of their degree of specificity for binding TFIIIA compared to other zinc finger proteins (*31*). RNA1 exhibited a complete lack of specificity for TFIIIA, binding with subnanomolar to nanomolar affinities to all of the C_2H_2 zinc finger proteins tested. RNA21 demonstrated intermediate specificity, binding with its highest affinity to TFIIIA and p43, with 10−100-fold lower affinity for several unrelated zinc finger proteins and having no affinity for

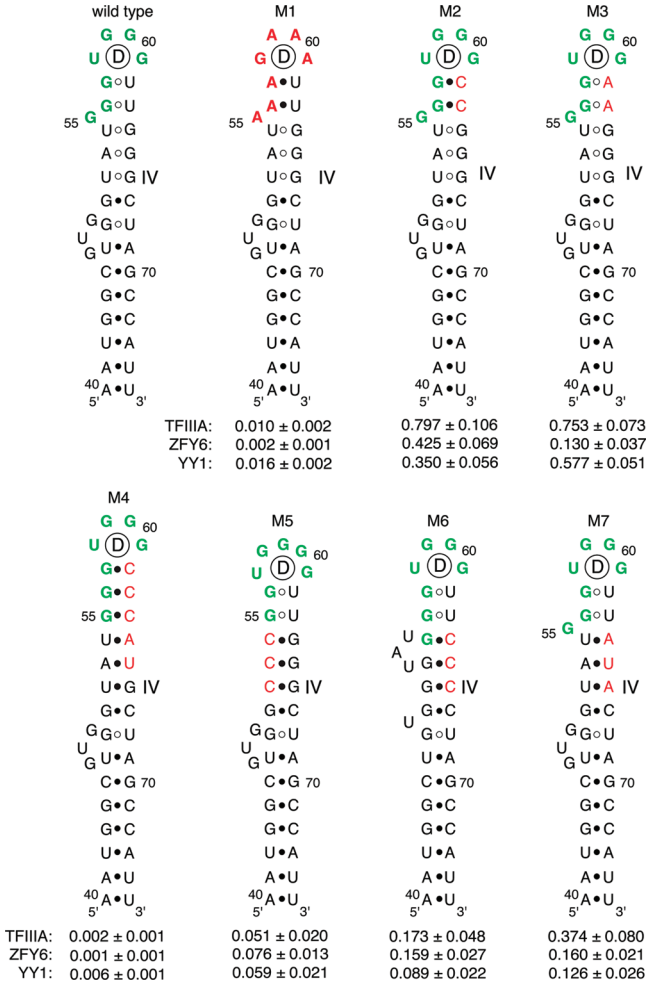

FIGURE 6: Effects of site-directed mutations of RNA1 on the binding of TFIIIA, ZFY6, and YY1. For the sake of clarity, only the region from nucleotide 40 to 75 of RNA1 is shown. The consensus sequence is colored green, and nucleotide changes are colored red. The relative affinities of each protein for each mutant RNA1 are shown below and represent the mean of three independent determinations reported with the associated errors (Materials and Methods).

the other zinc finger proteins tested. Only the RNA22 aptamer exhibited specificity for TFIIIA and p43 congruent with the specificity of these proteins for their biological ligand, 5S rRNA.

To understand the similarities and differences in the zinc finger binding properties of these three RNA aptamers, the effects of different equilibrium binding conditions on TFIIIA binding affinity were compared. The most distinctive differences were observed in the responses to changes in pH and assay temperature. Changing the pH of the assay buffer and measuring the effects on the apparent K_a provide information about the importance of titratable groups on both the RNA and the protein that are involved in forming contacts that promote formation of the RNA−protein complex. The pH profile was distinct for each of the three aptamers. The pH profile for RNA22 is remarkably similar to the pH profile for the binding of 5S rRNA to TFIIIA (*31*), consistent with the high degree of specificity RNA22 has for TFIIIA and the functionally related protein p43. The broader pH optimum of the RNA21 aptamer may be related to its ability to bind a more diverse group of zinc finger proteins that RNA22 does. The most interesting pH profile was that observed for the binding of TFIIIA to RNA1. The highest affinity of RNA1 for TFIIIA was measured at the lowest pH tested, with the affinity gradually decreasing as the pH increased. This result suggests that at least one titratable group on either RNA1 or TFIIIA with a pK_a value of ≤6.0 is critical for formation of the RNA−protein complex.

The contribution of enthalpy and entropy to the free energy of binding TFIIIA was also compared for all three aptamers. At the assay temperature of 20 °C, formation of the TFIIIA−RNA1 complex is driven by a large, favorable entropy with little contribution from enthalpy. In comparison, formation of the RNA21−TFIIIA and RNA22−TFIIIA complexes is driven by large, favorable enthalpy terms, while the entropy terms for both interactions are unfavorable. These two interactions can also be distinguished from the RNA1−TFIIIA interaction because they have temperature-dependent enthalpies. The fact that the RNA1−TFIIIA complex is favored by entropy is consistent with the release of more water molecules and counterions from both the RNA and the protein than occurs in the formation of the other two aptamer−TFIIIA complexes. More water molecules would be released if the interaction surface within the RNA1−TFIIIA complex is larger than the interaction surfaces in the other two aptamer−TFIIIA complexes.

The interactions of the broad-specificity RNA1 aptamer and the highly specific RNA22 aptamer with TFIIIA can also be distinguished on the basis of the effects of site directed mutations of the protein. Heterologous replacement of amino acid sequences in fingers 4 and 6 of TFIIIA with sequences from the unrelated protein WT1 results in a significant loss of binding to RNA22, as expected for such a highly specific interaction that mimics the biological TFIIIA−5S rRNA interaction. In contrast, the same battery of chimeric TFIIIA mutations have only modest effects on the interaction with RNA1, in most cases resulting in a slight increase in affinity, consistent with the ability of this aptamer to bind to a broad range of zinc finger proteins.

We also investigated the similarities and differences in the binding of three zinc finger proteins to RNA1, using TFIIIA with nine zinc fingers, an eight-finger peptide derived from the ZFY protein (ZFY6), and the four-zinc finger domain from the YY1 protein. All three proteins bind to RNA1 with high affinity in a zinc-dependent manner, with dissociation constants ranging from 0.24 to 5.3 nM. The general effects of increasing monovalent and divalent salt concentrations on the binding of these three proteins to RNA1 are quite similar. The interaction of RNA1 with TFIIIA is distinctly different from its interaction with either ZFY6 or YY1 in its response to changes in the pH of the assay buffer. Although all three proteins exhibit the same trend of peaking at an optimum of pH ≤6.0, ZFY6 and YY1 show a significant decrease in affinity for RNA1 at pH >7.5, while the affinity of TFIIIA for RNA1 is essentially the same from pH 7.5 to 9.0. This result indicates that a group with a pK_a value of around 8.0 on RNA1 or on ZFY6 and YY1 is essential for formation of a complex between the RNA and these two zinc finger proteins.

The interactions of YY1 and ZFY6 with RNA1 can also be distinguished from the TFIIIA interaction on the basis of relative contributions of enthalpy and entropy to the free energy of complex formation. The TFIIIA−RNA1 interaction is driven by a large favorable entropy, with enthalpy making little or no contribution. In comparison, the interactions of both YY1 and ZFY6 with RNA1 are driven by favorable enthalpy terms, indicating that there are multiple mechanistic routes to forming a high-affinity zinc finger complex with RNA1.

The secondary structure predicted for RNA1 places the GGGUGGG consensus sequence in a hairpin loop at the end

of a long helical arm with noncanonical base pairs closing the hairpin loop. Mutagenesis of this region of RNA1 confirmed the importance of the GGGUGGG sequence, and its structural context, for binding of zinc finger proteins. These results suggest that the GGGUGGG region of RNA1 provides the key nucleation point for the interaction of a zinc finger protein with RNA1 and would probably interact with one or two zinc fingers. The overall free energy of binding increases 0.282 kcal/mol for each additional zinc finger in a protein, consistent with the formation of at least one noncovalent bond between each additional finger and RNA1. This consistent increase in free energy per additional zinc finger implies that all zinc fingers brought into the proximity of RNA1 after the nucleation event are in a configuration that allows for bonding interactions to occur. Either there is a preformed complementary binding surface between the zinc finger proteins and RNA1, or an induced fit between RNA1 and each zinc finger protein may occur upon binding.

The zinc finger−RNA1 binding data are consistent with a simple bimolecular equilibrium. Attempts to confirm the 1:1 stoichiometry of these complexes by gel shift analysis were unsuccessful because the complexes dissociate during electrophoresis. The consistent increase in binding free energy with each additional zinc finger for proteins with three to nine fingers and the absolute requirement for the GGGUGGG motif in RNA1 are consistent with the formation of 1:1 complexes between the aptamer and the zinc finger proteins that is nucleated at the GGGUGGG hairpin. In the three-dimensional structure of a complex consisting of zinc fingers 4−6 of TFIIIA bound to a 61-nucleotide truncated version of the 5S rRNA, the interaction surface between the protein and RNA is approximately 40 Å long, within an overall peptide length of 69 Å and an overall length of 80 Å for the truncated 5S rRNA (*30*). A rough estimate based on those parameters suggests that the overall length of the 95-nucleotide RNA1 would be 120 Å, which would accommodate approximately five or six zinc fingers. Since the free energy of binding to RNA1 continues to increase for proteins with seven to nine zinc fingers, the mode of interaction between RNA1 and zinc finger proteins is likely different from the mode of the TFIIIA−5S rRNA interaction.

It was originally hypothesized that the outcome of a selection for ligands with high affinities for a target protein would result in ligands that also had high specificity for that target (*48*). "Generalist" RNA aptamers with high affinity for more than one protein were first isolated in a study of MS2 and Qβ phage coat proteins (*49*). Since the two coat proteins have limited sequence identity and bind to RNA hairpins that differ significantly in sequence and structure, this result was unexpected but resulted from a structure in the aptamers that bound to coat protein dimers rather than monomers. Several groups of generalist RNA aptamers were also isolated in selection experiments conducted in parallel with two unrelated double-stranded RNA binding domains (dsRBD) (*50*). This result was not unexpected, since dsRBD proteins bind to RNA in a sequence-independent fashion, any specificity in the interaction relying upon the formation of specific structures in the RNA (*51*). In comparison to these previous studies, RNA1 is novel as a generalist RNA aptamer for having high affinity for all members of a class of nucleic acid binding proteins.

The properties of the RNA1 and RNA21 aptamers isolated from the random library by TFIIIA raise some interesting questions about the interaction of zinc finger proteins with RNA in the cellular environment. The selection of these aptamers suggests the possibility that like dsRBD proteins, zinc finger proteins may have an inherent ability to bind to RNA in a high-affinity, nonselective fashion. The properties of the RNA1 and RNA21 aptamers suggest that biological RNAs that have the ability to bind to more than one zinc finger protein with high affinity could exist. A biological RNA with properties similar to those of RNA21 might serve as a staging point, or sequestration agent, for a limited number of zinc finger proteins, allowing for coordinated release of the proteins on a specific time scale, or release in a specific cellular location. The identification and characterization of biological RNA molecules with high affinity for a subset of zinc finger proteins should lead to new insights into the cellular mechanisms of this class of proteins.

ACKNOWLEDGMENT

We thank Jill Turner and Ioana Rosu for technical assistance.

REFERENCES

1. Laity, J. H., Lee, B. M., and Wright, P. E. (2001) Zinc finger proteins: New insights into structural and functional diversity. *Curr. Opin. Struct. Biol. 11*, 39–46.
2. Ladomery, M., and Dellaire, G. (2002) Multifunctional zinc finger proteins in development and disease. *Ann. Hum. Genet. 66*, 331–342.
3. Bogenhagen, D. F., Sakonju, S., and Brown, D. D. (1980) A control region in the center of the 5S RNA gene directs specific initiation of transcription: II. The 3′ border of the region. *Cell 19*, 27–35.
4. Engelke, D. R., Ng, S.-Y., Shastry, B. S., and Roeder, R. G. (1980) Specific interaction of a purified transcription factor with an internal control region of 5S RNA genes. *Cell 19*, 717–728.
5. Sakonju, S., Bogenhagen, D. F., and Brown, D. D. (1980) A control region in the center of the 5S RNA gene directs specific initiation of transcription: I. The 5′ border of the region. *Cell 19*, 13–25.
6. Sakonju, S., Brown, D. D., Engelke, D., Ng, S.-Y., Shastry, B. S., and Roeder, R. G. (1981) The binding of a transcription factor to deletion mutants of a 5S rRNA gene. *Cell 23*, 665–669.
7. Picard, B., and Wegnez, M. (1979) Isolation of a 7S particle from *Xenopus laevis* oocytes: A 5S RNA-protein complex. *Proc. Natl. Acad. Sci. U.S.A. 76*, 241–245.
8. Honda, B. M., and Roeder, R. G. (1980) Association of a 5S gene transcription factor with 5S RNA and altered levels of the factor during cell differentiation. *Cell 22*, 119–126.
9. Pelham, H. R. B., and Brown, D. D. (1980) A specific transcription factor that can bind either the 5S RNA gene or 5S RNA. *Proc. Natl. Acad. Sci. U.S.A. 77*, 4170–4174.
10. Denis, H., and le Maire, M. (1983) Thesaurisomes, a novel kind of nucleoprotein particle. *Subcell. Biochem. 9*, 263–297.
11. Clemens, K. R., Liao, X. B., Wolf, V., Wright, P. E., and Gottesfeld, J. M. (1992) Definition of the binding sites of individual zinc fingers in the transcription factor IIIA-5S RNA gene complex. *Proc. Natl. Acad. Sci. U.S.A. 89*, 10822–10826.
12. Darby, M. K., and Joho, K. E. (1992) Differential binding of zinc fingers from *Xenopus* TFIIIA and p43 to 5S RNA and the 5S RNA gene. *Mol. Cell. Biol. 12*, 3155–3164.
13. Hayes, J. J., and Clemens, K. R. (1992) Locations of contacts between individual zinc fingers of *Xenopus laevis* transcription factor IIIA and the internal control region of a 5S RNA gene. *Biochemistry 31*, 11600–11605.
14. Liao, X. B., Clemens, K. R., Tennant, L., Wright, P. E., and Gottesfeld, J. M. (1992) Specific interaction of the first three zinc fingers of TFIIIA with the internal control region of the *Xenopus* 5S RNA gene. *J. Mol. Biol. 223*, 857–871.
15. Theunissen, O., Rudt, F., Guddat, U., Mentzel, H., and Pieler, T. (1992) RNA and DNA binding zinc fingers in *Xenopus* TFIIIA. *Cell 71*, 679–690.
16. Clemens, K. R., Wolf, V., Mcbryant, S. J., Zhang, P. H., Liao, X. B., Wright, P. E., and Gottesfeld, J. M. (1993) Molecular basis for specific recognition of both RNA and DNA by a zinc finger protein. *Science 260*, 530–533.
17. Del Rio, S., Menezes, S. R., and Setzer, D. R. (1993) The function of individual zinc fingers in sequence specific DNA recognition by transcription factor IIIA. *J. Mol. Biol. 233*, 567–579.
18. Clemens, K. R., Zhang, P. H., Liao, X. B., McBryant, S. J., Wright, P. E., and Gottesfeld, J. M. (1994) Relative contributions of the zinc

fingers of transcription factor IIIA to the energetics of DNA binding. *J. Mol. Biol. 244*, 23–35.
19. McBryant, S. J., Veldhoen, N., Gedulin, B., Leresche, A., Foster, M. P., Wright, P. E., Romaniuk, P. J., and Gottesfeld, J. M. (1995) Interaction of the RNA binding fingers of *Xenopus* transcription factor IIIA with specific regions of 5 S ribosomal RNA. *J. Mol. Biol. 248*, 44–57.
20. Setzer, D. R., Menezes, S. R., Del Rio, S., Hung, V. S., and Subramanyan, G. (1996) Functional interactions between the zinc fingers of *Xenopus* transcription factor IIIA during 5S rRNA binding. *RNA 2*, 1254–1269.
21. Wuttke, D. S., Foster, M. P., Case, D. A., Gottesfeld, J. M., and Wright, P. E. (1997) Solution structure of the first three zinc fingers of TFIIIA bound to the cognate DNA sequence determinants of affinity and sequence specificity. *J. Mol. Biol. 273*, 183–206.
22. Ryan, R. F., and Darby, M. K. (1998) The role of zinc finger linkers in p43 and TFIIIA binding to 5S rRNA and DNA. *Nucleic Acids Res. 26*, 703–709.
23. Stoll, R., Lee, B. M., Debler, E. W., Laity, J. H., Wilson, I. A., Dyson, H. J., and Wright, P. E. (2007) Structure of the Wilms tumor suppressor protein zinc finger domain bound to DNA. *J. Mol. Biol. 372*, 1227–1245.
24. Weiss, T. C., and Romaniuk, P. J. (2009) Contribution of individual amino acids to the RNA binding activity of the Wilms' tumor suppressor protein WT1. *Biochemistry 48*, 148–155.
25. Kuwabara, T., Hsieh, J., Nakashima, K., Taira, K., and Gage, F. H. (2004) A small modulatory dsRNA specifies the fate of adult neural stem cells. *Cell 116*, 779–793.
26. Finerty, P. J., Jr., and Bass, B. L. (1997) A *Xenopus* zinc finger protein that specifically binds dsRNA and RNA-DNA hybrids. *J. Mol. Biol. 271*, 195–208.
27. Finerty, P. J., Jr., and Bass, B. L. (1999) Subsets of the zinc finger motifs in dsRBP-ZFa can bind double-stranded RNA. *Biochemistry 38*, 4001–4007.
28. Möller, H. M., Martinez-Yamout, M. A., Dyson, H. J., and Wright, P. E. (2005) Solution structure of the N-terminal zinc fingers of the *Xenopus laevis* double stranded RNA binding protein ZFa. *J. Mol. Biol. 351*, 718–730.
29. Brown, R. S. (2005) Zinc finger proteins: Getting a grip on RNA. *Curr. Opin. Struct. Biol. 15*, 94–98.
30. Lu, D., Searles, M. A., and Klug, A. (2003) Crystal structure of a zinc finger-RNA complex reveals two modes of molecular recognition. *Nature 426*, 96–100.
31. Weiss, T. C., Zhai, G. G., and Romaniuk, P. J. (2010) An RNA Aptamer with High Affinity and High Specificity for the 5S RNA Binding Zinc Finger Proteins TFIIIA and p43. *Biochemistry 49*, 1755–1765.
32. Hamilton, T., Barilla, K., and Romaniuk, P. (1995) High affinity binding sites for the Wilms' tumour suppressor protein WT1. *Nucleic Acids Res. 23*, 277–284.
33. Veldhoen, N., You, Q. M., Setzer, D. R., and Romaniuk, P. J. (1994) Contribution of individual base pairs to the interaction of TFIIIA with the *Xenopus* 5S RNA gene. *Biochemistry 33*, 7568–7575.
34. Zang, W. Q., and Romaniuk, P. J. (1995) Characterization of the 5S RNA binding activity of *Xenopus* zinc finger protein p43. *J. Mol. Biol. 245*, 549–558.
35. Bradford, M. M. (1976) A rapid and sensitive method for the quantitation of microgram quantities of protein utilizing the principle of protein-dye binding. *Anal. Biochem. 72*, 248–254.
36. Zhai, G., Iskandar, M., Barilla, K., and Romaniuk, P. J. (2001) Characterization of RNA aptamer binding by the Wilms' tumor suppressor protein WT1. *Biochemistry 40*, 2032–2040.
37. Hall, K. B., and Kranz, J. K. (1999) Nitrocellulose filter binding for determination of dissociation constants. *Methods Mol. Biol. 118*, 105–114.
38. Ha, J. H., Spolar, R. S., and Record, M. T., Jr. (1989) Role of the hydrophobic effect in stability of site-specific protein-DNA complexes. *J. Mol. Biol. 209*, 801–816.
39. Record, M. T., Jr., Lohman, T. M., and de Haseth, P. (1976) Ion effects on ligand-nucleic acid interactions. *J. Mol. Biol. 107*, 145–158.
40. Record, M. T., Jr., Anderson, C. F., and Lohman, T. M. (1978) Thermodynamic analysis of ion effects on the binding and conformational equilibria of proteins and nucleic acids: The roles of ion association or release, screening, and ion effects on water activity. *Q. Rev. Biophys. 11*, 103–178.
41. Lohman, T. M., deHaseth, P. L., and Record, M. T., Jr. (1980) Pentalysine-deoxyribonucleic acid interactions: A model for the general effects of ion concentrations on the interactions of proteins with nucleic acids. *Biochemistry 19*, 3522–3530.
42. Misra, V. K., and Draper, D. E. (1998) On the role of magnesium ions in RNA stability. *Biopolymers 48*, 113–135.
43. Gerstner, R. B., Pak, Y., and Draper, D. E. (2001) Recognition of 16S rRNA by ribosomal protein S4 from *Bacillus stearothermophilus*. *Biochemistry 40*, 7165–7173.
44. Drygin, D., and Zimmermann, R. A. (2000) Magnesium ions mediate contacts between phosphoryl oxygens at positions 2122 and 2176 of the 23S rRNA and ribosomal protein L1. *RNA 6*, 1714–1726.
45. Hamilton, T. B., Turner, J., Barilla, K., and Romaniuk, P. J. (2001) Contribution of individual amino acids to the nucleic acid binding activities of the *Xenopus* zinc finger proteins TFIIIA and p43. *Biochemistry 40*, 6093–6101.
46. Zang, W. Q., Veldhoen, N., and Romaniuk, P. J. (1995) Effects of zinc finger mutations on the nucleic acid binding activities of *Xenopus* transcription factor IIIA. *Biochemistry 34*, 15545–15552.
47. Wimberly, B., Varani, G., and Tinoco, I. (1993) The conformation of loop E of eukaryotic 5S ribosomal RNA. *Biochemistry 32*, 1078–1087.
48. Eaton, B. E., Gold, L., and Zichi, D. A. (1995) Let's get specific: The relationship between specificity and affinity. *Chem. Biol. 2*, 633–638.
49. Hirao, I., Spingola, M., Peabody, D., and Ellington, A. D. (1998) The limits of specificity: An experimental analysis with RNA aptamers to MS2 coat protein variants. *Mol. Diversity 4*, 75–89.
50. Hallegger, M., Taschner, A., and Jantsch, M. F. (2006) RNA aptamers binding the double stranded RNA binding domain. *RNA 12*, 1993–2004.
51. Bass, B. L. (2002) RNA editing by adenosine deaminases that act on RNA. *Annu. Rev. Biochem. 71*, 817–846.
52. Zuker, M. (1989) On finding all suboptimal foldings of an RNA molecule. *Science 244*, 48–52.
53. Mathews, D. H., Sabina, J., Zuker, M., and Turner, D. H. (1999) Expanded sequence dependence of thermodynamic parameters improves prediction of RNA secondary structure. *J. Mol. Biol. 288*, 911–940.